Colloids and Surfaces A: Physicochem. Eng. Aspects 367 (2010) 96–101

Contents lists available at ScienceDirect

Colloids and Surfaces A: Physicochemical and Engineering Aspects

journal homepage: www.elsevier.com/locate/colsurfa

# A one-step facile synthesis of Ag–Ni core–shell nanoparticles in water-in-oil microemulsions

Lixin Xia[a,*], Xinhu Hu[a], Xiaobo Kang[a], Hongping Zhao[a], Mengtao Sun[b], Xiaowei Cihen[c]

[a] College of Chemistry, Liaoning University, 66 Chongshan Middle Road, Huanggu District, Shenyang 110036, China
[b] Beijing National Laboratory for Condensed Matter Physics, Institute of Physics, Chinese Academy of Sciences, Beijing 100190, China
[c] Departamento de Ciencia de los Materiales, Ingeniería Metalúrgicay Química Inorgánica, Facultad de Ciencias, Universidad de Cádiz (Campus Río San Pedro), E-11510 Puerto Real (Cádiz), Spain

ARTICLE INFO

*Article history:*
Received 15 April 2010
Received in revised form 22 June 2010
Accepted 23 June 2010
Available online 3 July 2010

*Keywords:*
One-step synthesis
Bimetallic nanoparticle
Core–shell structure
Nickel
Silver

ABSTRACT

A one-step facile synthesis is devised for preparation of well-dispersed Ag–Ni core–shell nanoparticles with uniform and intact shells. The process is performed by a reduction of silver nitrate and nickel nitrate with sodium borohydride in water-in-oil (W/O) microemulsions of water/polyoxyethylene (4) nonylphenol (OP-4) and polyoxyethylene (7) nonylphenol (OP-7)/*n*-heptane. Transmission electron microscopy (TEM), X-ray diffraction (XRD), X-ray photoelectron spectroscopy (XPS), and UV–vis absorption are utilized to characterize the Ag–Ni core–shell nanoparticles. Furthermore, the effect of molar ratio of $Ni^{2+}$ to $Ag^{+}$ and dosage of $Ni^{2+}$ and $Ag^{+}$ on morphology of the core–shell nanostructure is also discussed in detail. The thickness of Ni layers on the surface of Ag nanoparticles could be controlled by the dosage of $Ni^{2+}$ and $Ag^{+}$. The Ag–Ni core–shell nanoparticles showed a high catalytic activity for degradation reaction of eosin Y. The product may also have many potential applications in optical, magnetic, biochemical, and biomedical fields. The synthetic method reported here suggests a very promising route for the preparation of bimetallic core–shell structures, which is a subject of intense interest.

## 1. Introduction

Since nanoparticles usually exhibit unusual electronic, optical, magnetic, and chemical properties significantly different from those of the bulk materials due to their extremely small sizes and large specific surface areas, they have various applications such as catalysis, electronic, optical, mechanic devices, magnetic recording media, superconductors, high-performance engineering materials, dyes, pigments, adhesives, photographic suspensions, drug delivery, and so on [1–15]. Especially in recent years, nano-sized core–shell bimetallic particles have received much attention due to their superior optical, electronic, catalytic, and magnetic properties compared to their monometallic counterparts [16]. These interesting physicochemical properties result from the combination of two kinds of metals and their fine structures, evolving new surface characteristics [17]. Successive reduction of one metal after another is normally employed to produce a core–shell structure [17–21], but such particles are not always generated [22]. On the other hand, nanoparticles synthesized by the co-reduction of two kinds of metal ions often leads to alloyed nanoparticles, although core–shell structures have also been observed [20,23–26]. In addition, stable small Ag–Ni alloy nanoparticles were recently synthesized by a radiolytic approach, and these nanoparticles were identified to be not core–shell structure [27]. Therefore, synthesis of bimetallic core–shell particles with sizes in the nanometer range requires a great deal of control over the synthetic technique.

Nickel has been known to be one of the important catalytic, magnetic, and conductive materials. Very recently, Bala et al. prepared the oleic acid-capped Ni–Ag core–shell nanoparticles in the aqueous foams [28], and Chen et al. prepared Ni–Ag core–shell nanoparticles by successive hydrazine reduction in ethylene glycol [17,18]. Goodman reported that the Pt–Ni surfaces, with Ni coverages in the monolayer regime, showed higher hydrogenolysis activity than that on either Ni or Pt [16].

Water-in-oil (W/O) microemulsion solutions are transparent, isotropic liquid media with nano-sized water droplets that are dispersed in a continuous oil phase and stabilized by surfactant molecules at the water/oil interface. These surfactant-covered water pools offer a unique microenvironment for the formation of nanoparticles. They not only act as microreactors for processing reactions but also inhibit the excess aggregation of particles because the surfactants could adsorb on the particle surface when the particle size approaches to that of water pool. As a result, the particles obtained in such a medium are generally very fine and monodispersed [29].

---

* Corresponding author. Tel.: +86 24 62202393; fax: +86 24 62202139.
*E-mail address:* lixinxia@lnu.edu.cn (L. Xia).

0927-7757/$ – see front matter © 2010 Elsevier B.V. All rights reserved.
doi:10.1016/j.colsurfa.2010.06.020

**Scheme 1.** Proposed procedure of the one-step synthesis of Ag–Ni core–shell nanoparticles in W/O microemulsions.

Herein, we report Ag–Ni core–shell nanoparticles was synthesized by a one-step reduction of silver nitrate and nickel nitrate with sodium borohydride in W/O microemulsions of water/OP-4 and OP-7/*n*-heptane. The size and structure of the resultant core–shell nanoparticles were characterized by TEM, XRD, XPS, and UV–vis absorption. Furthermore, effect of dosage of nickel nitrate and silver nitrate on morphology of the core–shell nanostructure was investigated and discussed. In addition, catalytic property of the as-synthesized Ag–Ni core–shell nanoparticles for degradation reaction of eosin Y was also investigated.

## 2. Experimental

### 2.1. Materials

Nickel nitrate hexahydrate (≥98%) was the product of Xinxi Chemical Reagent Factory, Shenyang, China. Silver nitrate (>99.8%) was purchased from Junsei Chemical Co., Ltd. *n*-Heptane (≥98.5%) was supplied by Regent Chemicals Co., Ltd., Tianjin, China. Sodium hydroxide (≥96%) and sodium borohydride (≥96%) were acquired from Sinopharm Chemical Reagent Co., Ltd., China. Ammonia solution (28.0–30.0%) was obtained from Sanchun Pure Chemical Co., Ltd. The surfactants, OP-4 and OP-7, were obtained from Liaoyang Aoke Chemical Company, China, and eosin Y (99%) was purchased from Alfa Aesar. Other chemicals, unless specified, were of reagent grade and used without further purification. High purity water with resistivity >18.0 MΩ cm was used in all preparations.

### 2.2. Preparation of Ni–Ag core–shell nanoparticles

Two microemulsion solutions were prepared as follows: 1 drop of 10 wt% sodium hydroxide aqueous solution was added to a mixture of nickel nitrate and silver nitrate (in a molar ratio of 2:1) aqueous solutions to form fine precipitates of $Ag_2O$ and $Ni(OH)_2$. Ammonia solution (8 wt%) was added drop by drop to this mixture until the precipitates completely dissolved to form $[Ag(NH_3)_2]^+$ and $[Ni(NH_3)_6]^{2+}$, then pure water was added until the solution weight was up to 1 g. Subsequently, 1.75 g of OP-4, 11.00 g of *n*-heptane, 0.70 g of OP-7 was weighed and then poured, under continuous mechanical stirring, into the above $[Ag(NH_3)_2]^+$ and $[Ni(NH_3)_6]^{2+}$solution, and remained for 30 min in water-bath at 25 °C. The transparent microemulsion solution was obtained and named as microemulsion A. Replacing the $[Ag(NH_3)_2]^+$ and $[Ni(NH_3)_6]^{2+}$solution by 1 g of 2.5 wt% sodium borohydride aqueous solution with the other conditions kept as constant, the obtained microemulsion solution was named as microemulsion B.

The microemulsion A was dropwise added into the microemulsion B, and then the whole mixture was left to react for 1 h in water-bath at 25 °C under continuous mechanical stirring. The products were collected by centrifugation and washed several times with water and anhydrous ethanol, and then dried under vacuum at room temperature for 4 h. The procedure for the experiment is depicted in Scheme 1.

### 2.3. Catalytic reduction process

In a representative reduction experiment, 1 mg of the Ni–Ag core–shell nanoparticles were mixed with 1 mL of eosin Y aqueous solution ($4 \times 10^{-5}$ mol L$^{-1}$). After that, 1 mL of freshly prepared $NaBH_4$ aqueous solution ($4 \times 10^{-2}$ mol L$^{-1}$) was rapidly added into the above mixture. The color of the mixture gradually vanished, indicating the reduction of the dye.

### 2.4. Characterization

The microstructure and size of the core–shell nanoparticles were obtained by TEM using a JEM-100SX instrument. TEM samples were prepared by drying aqueous suspensions of the particles on carbon-coated TEM grids under ambient conditions. XRD patterns of the core–shell nanoparticles were recorded with a D8ADVANCE powder diffractometer over a 2-theta range of 30–90° at an angular resolution of 0.02°. XPS measurements were carried out with ESCALAB 200 IXL spectrometer with a monochromatic X-ray source of Al Kα (1486.6 eV). UV–vis absorption spectra were measured at room temperature on a VARIAN Cary-5000 spectrophotometer using solutions in a 1 cm quartz cuvette.

## 3. Results and discussion

When the dosage of $Ni^{2+}$ and $Ag^+$ was 0.1 mmol and 0.05 mmol, a typical TEM micrograph and the size distributions for the core–shell nanoparticles obtained by a one-step reduction method in the W/O microemulsions were shown in Fig. 1(a). In the micrograph the particles are clearly spherical with diameters ranging from 50 nm to 100 nm. One of the more noteworthy features on the micrograph is the presence of the shell structure revealed as concentric rings on the particles. It is believed that $[Ag(NH_3)_2]^+$ can be preferentially reduced by $NaBH_4$ because of higher standard electrode potentials of the $[Ag(NH_3)_2]^+/Ag$ pair than that of the $[Ni(NH_3)_6]^{2+}/Ni$ pair [30], suggesting that the single core (visible as a dark region) in the central part of every nanoparticle with diameters ranging from 40 nm to 90 nm is metal Ag. The well-closed ring (visible as a light region) with a uniform wall of about 2–10 nm in thickness is metal Ni. In addition, because metal Ni has a lower conductivity than metal Ag, the core–shell structure as shown in Fig. 1(a) can be concluded that the Ag nanoparticles are completely covered by Ni layer. Silver ions were reduced by sodium borohydride due to their stronger oxidation ability, acting thereafter as a seed for reducing of nickel ions to lead to the formation of a shell layer over the silver particles. Thus, hierarchical nanostructured core–shell particle was generated. The corresponding histogram of the particle size distribution was also shown in Fig. 1A. The dominant particle size is 75 nm, the frequency is 33%. Adjusting the dosage of $Ni^{2+}$ and $Ag^+$ down to 0.06 mmol and 0.03 mmol or up to 0.24 mmol and 0.12 mmol with the other conditions kept as constant, the resultant nanoparticles were shown in Fig. 1(b) and (c). When the dosage of $Ni^{2+}$ and $Ag^+$ was decreased to 0.06 mmol and 0.03 mmol, a core–shell structure can be also obtained as shown in Fig. 1(b). The nanoparticles are spherical with diameters ranging from 50 nm to 100 nm and are partially aggregated. It can be also seen from Fig. 1(b) that there exist small amount of core-free Ni nanoparti-

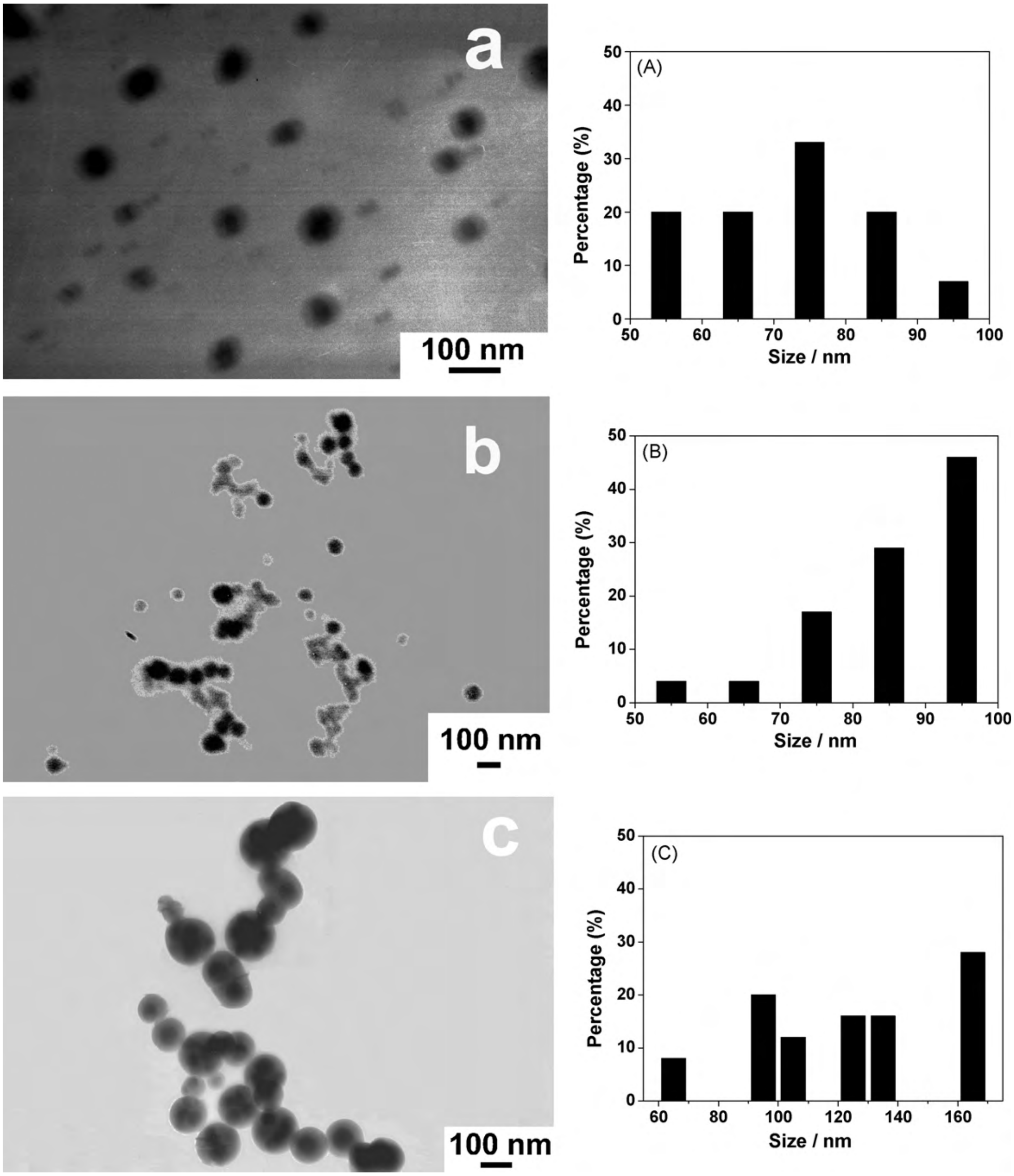

**Fig. 1.** TEM micrograph and size distribution of the core–shell nanoparticles. The dosage of $Ni^{2+}$ and $Ag^{+}$ is (a) 0.1 mmol and 0.05 mmol, (b) 0.06 mmol and 0.03 mmol, and (c) 0.24 mmol and 0.12 mmol, respectively. The corresponding histograms of the particle size distribution are indicated as A, B, and C.

cles and their aggregations. When the dosage of $Ni^{2+}$ and $Ag^{+}$ was increased to 0.24 mmol and 0.12 mmol, good core–shell structure was obtained as shown in Fig. 1(c). The thickness of the concentric rings on a single silver core increases up to the maximum value of 25 nm, and an around 60% proportion of the nanoparticles have multicore structure. Adjusting the dosage of $Ni^{2+}$ and $Ag^{+}$ down to 0.06 mmol and 0.03 mmol or up to 0.24 mmol and 0.12 mmol, the percentage of large size particles increased as shown in Fig. 1B and C. Compared with the dosage of $Ni^{2+}$ and $Ag^{+}$ of 0.1 mmol and 0.05 mmol, the particle size are bigger because the dominant particle size are 95 nm and 165 nm.

When the molar ratio of $Ni^{2+}$ and $Ag^{+}$ was varied to 1:1, 3:1, or 6:1 with 0.05 mmol dosage of $Ag^{+}$ and the other conditions kept unchanged, no good core–shell structure was observe (data not shown). The smaller dosage of $Ni^{2+}$ and $Ag^{+}$ led to the formation of small amount of core-free Ni nanoparticles and their aggregations, and the greater dosage of $Ni^{2+}$ and $Ag^{+}$ led to the formation of high proportion of multicore structure. Therefore, it can be concluded that the key factors for the preparation of core–shell nanoparticles in the water/OP-4 and OP-7/*n*-hexanol system seemed be the molar ratio of $Ni^{2+}$ to $Ag^{+}$ and the dosage of $Ni^{2+}$ and $Ag^{+}$. The thickness of Ni layers on the surface of Ag nanoparticles was controlled by the dosage of $Ni^{2+}$ and $Ag^{+}$. To the best of our knowledge, it is the first report to prepare core–shell nanoparticles by a one-step synthesis.

XRD measurements were performed on a D8ADVANCE powder diffractometer over a 2-theta range of 30–90° at an angular resolution of 0.02°. As shown in Fig. 2, four distinct diffraction peaks were clearly observed at $2\theta$ values of 38.18°, 64.60°, 77.50°, and 81.68°, corresponding to the reflections of the {1 1 1}, {2 2 0}, {3 1 1}, and {2 2 2} crystal planes, respectively, of the cubic structure of metallic

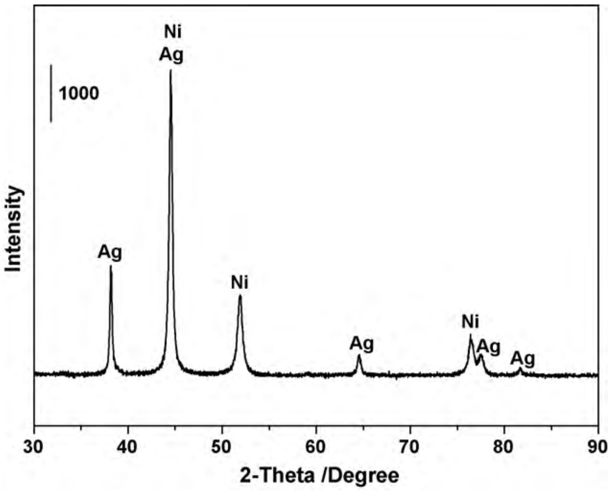

**Fig. 2.** Typical XRD patterns of Ag–Ni core–shell nanoparticles. The dosage of Ni$^{2+}$ and Ag$^+$ is 0.1 mmol and 0.05 mmol.

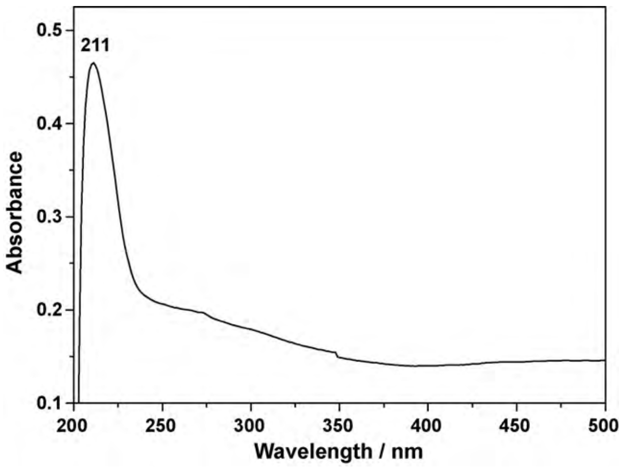

**Fig. 4.** UV–vis absorption spectrum of Ag–Ni core–shell nanoparticles. The dosage of Ni$^{2+}$ and Ag$^+$ is 0.24 mmol and 0.12 mmol.

Ag, which was in good agreement with the standard values given by the Joint Committee on Powder Diffraction Standards. In addition, the XRD analysis also revealed three main characteristic peaks for the $\{1\,1\,1\}$, $\{2\,0\,0\}$, and $\{2\,2\,0\}$ crystal planes of metallic Ni at $2\theta = 44.54^\circ$, $51.92^\circ$, and $76.40^\circ$ [31]. The characteristic peak for the $\{1\,1\,1\}$ plane of Ni at $2\theta = 44.54^\circ$ was possibly overlapped with that for the $\{2\,0\,0\}$ plane of Ag at $2\theta = 44.40^\circ$. So, it could be concluded that both Ag cores and Ni shells have an fcc structure. Although it is known that nickel is easily oxidized to be oxides or hydroxide by water, no oxides or hydroxide such as NiO, $Ni_2O_3$, and $Ni(OH)_2$ were observed from the phase analysis by XRD, indicating the formation of pure nickel of high crystalline quality. This might be due to the fact that the water confined in the microemulsion droplets usually has significantly lower activity than the bulk water because the average diameters of microemulsion droplets are very small [32]. As mentioned above, the shell thickness of Ni is about 2–10 nm, and XRD could penetrate up to 5 nm. Thus, X-ray could touch Ag core covered by thin Ni shell (<5 nm). Consequently, the XRD pattern shows the peak for both Ni and Ag.

To further confirm the status of Ni shells, XPS measurements were carried out with ESCALAB 200 IXL spectrometer with a monochromatic X-ray source of Al K$\alpha$ (1486.6 eV). The characteristic XPS peak of Ni metal ($Ni^0$) is known to appear at 852.7 eV and 870 eV [33]; hence, two strong peaks are identified at 852.5 eV and 869.6 eV, as shown in Fig. 3(b), ensuring the formation of Ni shells ($Ni^0$), in agreement with XRD analysis. A very weak C 1s peak at 284 eV is from a contamination hydrocarbon covering the sample surface. O 1s peak at 530 eV results from the adsorbed oxygen [34]. No XPS peaks for NiO, $Ni_2O_3$, and $Ni(OH)_2$ were found showing that the Ni shells were not oxidized to be oxides or hydroxide. A comparison of the relative areas of integrated intensity shows that the $Ni^0$ is predominant component of the outer surfaces of the as-synthesized core–shell nanoparticles; trace Ag, which results from the cores of the core–shell nanoparticles, is also recorded due to X-ray penetration.

Fig. 4 shows the UV–vis absorption spectrum of Ag–Ni core–shell nanoparticles obtained at $Ni^{2+}/Ag^+ = 0.24$ mmol and 0.12 mmol. We recall the fact that a plasmon absorption appears at about 402 nm for silver colloids [35], and the bimetallic colloids show only one absorption band at 211 nm. Therefore, it is presumed that the homogeneous Ni shell layer over the silver particles is formed without independent silver particles in the medium, which is consistent with the result obtained by TEM.

To investigate catalytic activity of the as-synthesized Ag–Ni core–shell nanoparticles, the catalyst was employed to the reduction of eosin Y in the presence of $NaBH_4$. The progress of the catalytic reduction of eosin Y can be easily followed by the decrease in absorbance at the eosin Y $\lambda_{max}$ with time. Fig. 5 shows the evolution of the UV–vis spectra of eosin Y during its catalytic reduction in the presence of the Ag–Ni core–shell nanoparticles. Evidently, the absorbance at $\lambda_{max}$ of eosin Y markedly decreases with the reaction time, which is indicative of the reduction of eosin Y. The reduction of the eosin Y by $NaBH_4$ is completed within 2 min in the solu-

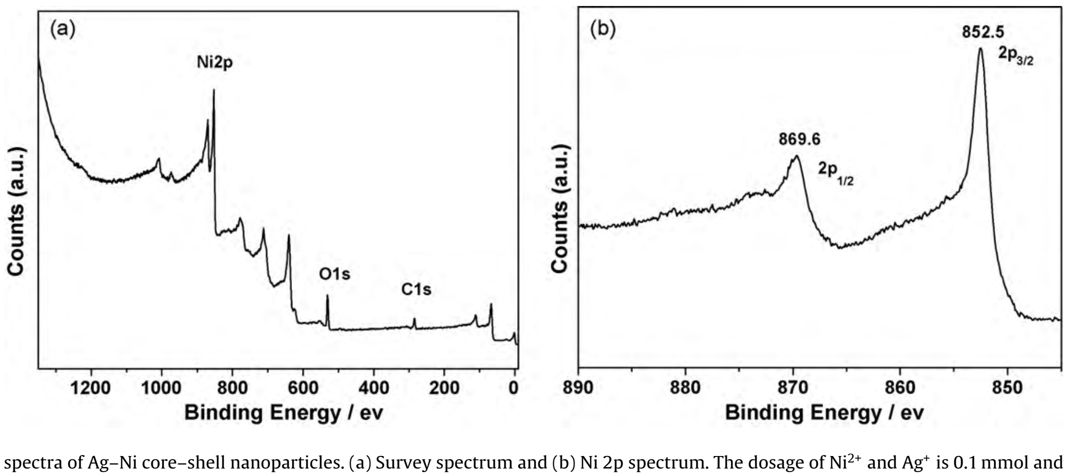

**Fig. 3.** XPS spectra of Ag–Ni core–shell nanoparticles. (a) Survey spectrum and (b) Ni 2p spectrum. The dosage of Ni$^{2+}$ and Ag$^+$ is 0.1 mmol and 0.05 mmol.

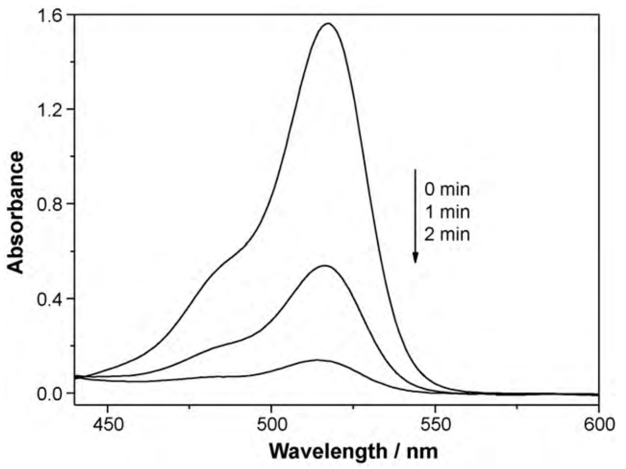

**Fig. 5.** UV–vis spectra of eosin Y during the reduction catalyzed with the Ag–Ni core–shell nanoparticles. $[NaBH_4] = 2 \times 10^{-2}$ mol L$^{-1}$ and [Eosin Y] $= 2 \times 10^{-5}$ mol L$^{-1}$. The arrows mark the increase of the reaction time.

tion containing the Ag–Ni core–shell nanoparticles. According to previous results [36–39], the reduction of eosin Y by $NaBH_4$ did not occur to an appreciable extent in the absence of appropriate catalyst. Therefore, it can be concluded that the Ag–Ni core–shell nanoparticles provided with high catalytic activity in the process of reducing eosin Y.

For comparison, the catalytic activity of pure Ag and Ni nanoparticles was also investigated. The pure Ag and Ni nanoparticles also exhibited high catalytic activity in the process of reducing eosin Y. Although the as-synthesized Ag–Ni core–shell nanoparticles did not showed better catalytic activity than those of pure Ag and Ni nanoparticles, the results demonstrate that it is possible to prepare bimetallic core–shell structures by using a one-step facile synthesis method. Further, the core–shell structure has the prominent advantage in avoiding the aggregation of the nanoparticles during the catalytic processes.

## 4. Conclusions

We have presented here a one-step facile method for preparation of Ag–Ni core–shell bimetallic nanoparticles. The synthesis of core–shell structures was accomplished by a reduction of silver nitrate and nickel nitrate with sodium borohydride in the W/O microemulsions of water/OP-4 and OP-7/*n*-heptane. Initially, silver ions were reduced by sodium borohydride due to their stronger oxidation ability, acting thereafter as a seed for reducing of Ni ions to lead to the formation of a shell layer over the silver particles. The key factors for the preparation of core–shell nanoparticles in the water/OP-4 and OP-7/*n*-hexanol system were the molar ratio of $Ni^{2+}$ to $Ag^+$ and the dosage of $Ni^{2+}$ and $Ag^+$. The thickness of Ni layers on the surface of Ag nanoparticles was controlled by the dosage of $Ni^{2+}$ and $Ag^+$. The analyses of XRD showed that the resultant shells were pure nickel crystalline of fcc structure. No oxides or hydroxide such as NiO, $Ni_2O_3$, and $Ni(OH)_2$ were observed. The as-synthesized Ag–Ni core–shell nanoparticles showed a high catalytic activity for degradation reaction of eosin Y, and may be found wider application in catalytic field. To the best of our knowledge, this is the first synthesis of bimetallic core–shell particles by using a one-step method. As long as standard electrode potentials of two type of metal ions is different or a kind of metal ion is modified by an appropriate complexing agent to make a gradient of standard electrode potentials with that of the other metal, the synthetical method may be applied to produce other bimetallic core–shell nanoparticles.

## Acknowledgments

We thank the financial supports from the Innovative Team Project of Department of Education of Liaoning Province, China (LT2010042), the Shenyang Natural Science Foundation, China (090082 and 2008gx–011), and the Liaoning University 211-Projects in the third period. Xiaowei Chen thanks "Ramóny Cajal" program from the Ministry of Science and Innovation of Spain.

## References

[1] J.H. Fendler, Atomic and molecular clusters in membrane mimetic chemistry, Chem. Rev. 87 (1987) 877–899.
[2] A. Henglein, Small-particle research: physicochemical properties of extremely small colloidal metal and semiconductor particles, Chem. Rev. 89 (1989) 1861–1873.
[3] V.L. Colvin, M.C. Schlamp, A.P. Alivisatos, Light-emitting diodes made from cadmium selenide nanocrystals and a semiconducting polymer, Nature 370 (1994) 354–357.
[4] J.F. Hamilton, R.C. Baetzold, Catalysis by small metal clusters, Science 205 (1979) 1213–1220.
[5] G. Schmid, Large clusters and colloids. Metals in the embryonic state, Chem. Rev. 92 (1992) 1709–1727.
[6] P.V. Kamat, Photochemistry on nonreactive and reactive (semiconductor) surfaces, Chem. Rev. 93 (1993) 267–300.
[7] L.N. Lewis, Chemical catalysis by colloids and clusters, Chem. Rev. 93 (1993) 2693–2730.
[8] B.C. Gates, Supported metal clusters: synthesis, structure, and catalysis, Chem. Rev. 95 (1995) 511–522.
[9] R.P. Andres, R.S. Averback, W.L. Brown, L.E. Brus, W.A. Goddard, A. Kaldor, S.G. Louie, M. Moscovits, P.S. Peercy, S.J. Riley, R.W. Siegel, F. Spaepen, Y. Wang, Research opportunities on clusters and cluster-assembled materials—a department of energy, council on materials science panel report, J. Mater. Res. 4 (1989) 704–736.
[10] L.L. Beecroft, C.K. Ober, Nanocomposite materials for optical applications, Chem. Mater. 9 (1997) 1302–1317.
[11] T. Yonezawa, N. Toshima, Mechanistic consideration of formation of polymer-protected nanoscopic bimetallic clusters, J. Chem. Soc., Faraday Trans. 91 (1995) 4111–4119.
[12] L. Brus, Electronic wave functions in semiconductor clusters: experiment and theory, J. Phys. Chem. 90 (1986) 2555–2560.
[13] A.J. Hoffman, G. Mills, H. Yee, M.R. Hoffmann, Q-sized cadmium sulfide: synthesis, characterization, and efficiency of photoinitiation of polymerization of several vinylic monomers, J. Phys. Chem. 96 (1992) 5546–5552.
[14] R.K. Hailstone, Computer simulation studies of silver cluster formation on AgBr microcrystals, J. Phys. Chem. 99 (1995) 4414–4428.
[15] A.F. Lee, C.J. Baddeley, C. Hardacre, R.M. Ormerod, R.M. Lambert, G. Schmid, H. West, Structural and catalytic properties of novel Au/Pd bimetallic colloid particles: EXAFS, XRD, and acetylene coupling, J. Phys. Chem. 99 (1995) 6096–6102.
[16] D.W. Goodman, Chemistry on monolayer metallic films, Ultramicroscopy 34 (1990) 1–9.
[17] D.H. Chen, S.R. Wang, Protective agent-free synthesis of Ni–Ag core–shell nanoparticles, Mater. Chem. Phys. 100 (2006) 468–471.
[18] C.C. Lee, D.H. Chen, Large-scale synthesis of Ni–Ag core–shell nanoparticles with magnetic, optical and anti-oxidation properties, Nanotechnology 17 (2006) 3094–3099.
[19] J.P. Wilcoxon, P.P. Provencio, Heterogeneous growth of metal clusters from solutions of seed nanoparticles, J. Am. Chem. Soc. 126 (2004) 6402–6408.
[20] M. Treguer, C. de Cointet, H. Remita, J. Khatouri, M. Mostafavi, J. Amblard, J. Belloni, R. de Keyzer, Dose rate effects on radiolytic synthesis of gold–silver bimetallic clusters in solution, J. Phys. Chem. B 102 (1998) 4310–4321.
[21] I. Srnová-Šloufová, B. Vlčková, Z. Bastl, T.L. Hasslett, Bimetallic (Ag)Au nanoparticles prepared by the seed growth method: two-dimensional assembling, characterization by energy dispersive X-ray analysis, X-ray photoelectron spectroscopy, and surface enhanced Raman spectroscopy, and proposed mechanism of growth, Langmuir 20 (2004) 3407–3415.
[22] J. Sinzig, U. Radtke, M. Quinten, U. Kreibig, Binary clusters: homogeneous alloys and nucleus–shell structures, Z. Phys. D 26 (1993) 242–245.
[23] B.K. Teo, K. Keating, Y.H. Kao, Observation of plasmon frequency in the optical spectrum of $Au_{18}Ag_{20}$ cluster: the beginning of the collective phenomenon characteristics of the bulk, J. Am. Chem. Soc. 109 (1987) 3494–3495.
[24] T. Itakura, K. Torigoe, K. Esumi, Preparation and characterization of ultrafine metal particles in ethanol by UV irradiation using a photoinitiator, Langmuir 11 (1995) 4129–4134.
[25] S.W. Han, Y. Kim, K. Kim, Dodecanethiol-derivatized Au/Ag bimetallic nanoparticles: TEM, UV/VIS, XPS, and FTIR analysis, J. Colloid Interface Sci. 208 (1998) 272–278.
[26] M.J. Hostetler, C.J. Zhong, B.K.H. Yen, J. Anderegg, S.M. Gross, N.D. Evans, M. Porter, R.W. Murray, Stable, monolayer-protected metal alloy clusters, J. Am. Chem. Soc. 120 (1998) 9396–9397.
[27] Z.Y. Zhang, T.M. Nenoff, J.Y. Huang, D.T. Berry, P.P. Provencio, Room temperature synthesis of thermally immiscible Ag–Ni nanoalloys, J. Phys. Chem. C 113 (2009) 1155–1159.

[28] T. Bala, S.D. Bhame, P.A. Joy, B.L.V. Prasad, M. Sastry, A facile liquid foam based synthesis of nickel nanoparticles and their subsequent conversion to $Ni_{core}Ag_{shell}$ particles: structural characterization and investigation of magnetic properties, J. Mater. Chem. 14 (2004) 2941–2945.

[29] B.K. Paul, S.P. Moulik, Microemulsions: an overview, J. Dispersion Sci. Technol. 18 (1997) 301–367.

[30] X. Lai, M. Xu, J. Fan, P. Guan, Handbook of Chemical Analysis, Science Press, Beijing, 1982 (in Chinese).

[31] D.E. Zhang, X.M. Ni, H.G. Zheng, Y. Li, X.J. Zhang, Z.P. Yang, Synthesis of needle-like nickel nanoparticles in water-in-oil microemulsion, Mater. Lett. 59 (2005) 2011–2014.

[32] D.H. Chen, S.H. Wu, Synthesis of nickel nanoparticles in water-in-oil microemulsions, Chem. Mater. 12 (2000) 1354–1360.

[33] F. Liu, J.Y. Lee, W. Zhou, Template preparation of multisegment PtNi nanorods as methanol electro-oxidation catalysts with adjustable bimetallic pair sites, J. Phys. Chem. B 108 (2004) 17959–17963.

[34] X. Peng, Y. Zhang, J. Zhao, F. Wang, Electrochemical corrosion performance in 3.5% NaCl of the electrodeposited nanocrystalline Ni films with and without dispersions of Cr nanoparticles, Electrochim. Acta 51 (2006) 4922–4927.

[35] S. Pande, S.K. Ghosh, S. Praharaj, S. Panigrahi, S. Basu, S. Jana, A. Pal, T. Tsukuda, T. Pal, Synthesis of normal and inverted gold–silver core–shell architectures in beta-cyclodextrin and their applications in SERS, J. Phys. Chem. C 111 (2007) 10806–10813.

[36] T. Pal, T.K. Sau, N.R. Jana, Silver hydrosol, organosol, and reverse micelle-stabilized sol—a comparative study, J. Colloid Interface Sci. 202 (1998) 30–36.

[37] N.R. Jana, T.K. Sau, T. Pal, Growing small silver particle as redox catalyst, J. Phys. Chem. B 103 (1999) 115–121.

[38] Z.J. Jiang, C.Y. Liu, L.W. Sun, Catalytic properties of silver nanoparticles supported on silica spheres, J. Phys. Chem. B 109 (2005) 1730–1735.

[39] F.X. Wang, M.W. Shao, L. Cheng, D.Y. Chen, Y. Fu, D.D.D. Ma, Si/Pd nanostructure with high catalytic activity in degradation of eosin Y, Mater. Res. Bull. 44 (2009) 126–129.